

THE DESCRIPTION OF WIGNER ENERGY AND ITS RELEASE FROM WINDSCALE PILE GRAPHITE FOR APPLICATION TO WASTE PACKAGING AND DISPOSAL

P.C. MINSHALL, A.J. WICKHAM
BNFL Magnox Generation,
Berkeley Centre, Berkeley
Gloucestershire,
United Kingdom

Abstract. The graphite core of Windscale Pile 1 is to be dismantled and packaged for interim storage, together with graphite items, such as dowels and boats from both Pile 1 and 2. These retain substantial amounts of Wigner energy and thus to support their packaging, storage and ultimate disposal, it is necessary to understand the release of the Wigner energy in slow, low temperature cycles, driven by the exothermic curing of the grout. The basic theories of the accumulation of Wigner energy and its release are reviewed. These show that the lattice defects introduced by neutron irradiation form a population of sites of different energies which is independent of the graphite type. The release of energy from each type of site can be described by a rate expression which is first order in the stored energy of the site, S , and has an associated activation energy, E , of decay. The overall rate of release, S , is given by a sum over the population of sites and has an effective lower limit determined by irradiation temperatures or post-irradiation conditions. In order to predict the release of Wigner energy activation energy spectra are derived from differential scanning calorimetry of samples of Windscale graphite. It is shown, by numerical solution of the release equation, that the derived spectra predict well both the experimental data and the release of energy from specimens derived from the same sample of Windscale graphite but subjected to different temperature cycles. Simulation of stored energy release in anticipated storage conditions, where the graphite is subjected to a slow temperature cycle driven by the exothermic curing of the grout, shows that only a small portion of the total stored energy is released. The slower the cycle, the greater the proportion of energy release, but the rate of release is slower.

1. INTRODUCTION

The graphite core of Windscale Pile 1 is to be dismantled, and the graphite packaged for interim storage in advance of disposal. There are also graphite items, mainly in the form of boats and dowels from both Pile 1 and Pile 2, in the waste in the B41 silo, that BNFL will recover and package. It is known from measurements on trepanned samples from the cores of Windscale Pile 1 and 2 (Refs [1] and [2]) that in general the graphite retains substantial amounts of Wigner energy, as do the boats and dowels (Ref. [3]) which resided in the channels through the core. In order to support a case for the waste packaging and disposal of Piles graphite, it is necessary to understand the behaviour of the residual Wigner energy under the relevant conditions, which routinely involve relatively low and slow temperature cycles. These cycles include those arising from the setting of grout used in packaging the waste in advance of eventual emplacement in a repository, from the setting of grout used to backfill repository vaults after waste emplacement, and from any long term radioactive decay heating. These are sufficiently different from reactor conditions that the recommended treatment of stored energy (Ref. [4]) does not give the requisite precision in describing the evolution of Wigner energy. This paper describes work undertaken to provide both a description of the Wigner energy in Piles graphite and the kinetics of its release.

2. BASIC THEORIES OF WIGNER ENERGY AND RELEASE

2.1 Classic Papers

Kelly (Ref. [5]) has provided a summary review of the theories of stored-energy release for general application in irradiated graphite. This discusses the various possibilities for the

kinetics of the release process, namely the constant activation energy model, the variable activation-energy model with a fixed frequency factor, and the variable frequency-factor model with a fixed activation energy, and expresses a preference for the variable activation-energy model with a fixed frequency factor. However, before examining this in detail it is useful to examine the fundamental published papers on which these arguments are based.

The classic paper is due to Vand (Ref. [6]) and is concerned with the stored energy in metallic films rather than graphite. It defines the basic energy-release equation, containing a

$$\frac{dN(E,t)}{dt} = -\nu N(E,t) \exp\left(-\frac{E}{kT}\right)$$

simple Boltzmann distribution term:

where N is the number of displacements per unit volume, ν is a constant “frequency factor”. E in the above equation is described as “decay energy” in early references but is, in fact, the activation energy for the decay process and not the difference in energies between the unstable

$$\nu = 4fn$$

and ground states of a particular defect. t is time. The frequency factor is given by where n is the number of atoms or vacancies forming the distortion (*i.e.* the cluster size) and $1/4f$ is the average time required for the initiation of the decay such that f is the “Debye maximum frequency” of the thermal oscillations of the lattice atoms. Vand queried the validity of taking the value of $1/4f$, which is representative of the pure material, and applying it to “distorted” areas of the lattice (*i.e.* to displaced atoms and vacancies). However, he showed that the release expression is far more sensitive to changes in the exponential term than to changes in n or f . ν may therefore vary between the several types of defect which may be present in the same sample of irradiated graphite.

T.J. Neubert was probably the first researcher to apply Vand’s theories to irradiation damage, working at Argonne National laboratory, but his work did not come to prominence until incorporated in the work of Primak (Ref. [7]) which looked very specifically at processes with distributions of activation energy.

Primak analysed the situation applicable to isothermal annealing in some detail. He

$$\Theta_n = \left[1 - \left((1-n) Bt \exp\left(-\frac{E}{kT}\right) \right) \right]^{1/n}$$

described a characteristic annealing function, Θ_n , given by for which a characteristic activation energy occurs when $\Theta_n = 1/e$. Here, $B = A(p/S_0)^{1-n}$ and, like A (a constant), has the dimensions of frequency. p , the importance factor, relates the change in stored energy to the change in the number of defects and n is the order of reaction (n.b. $\Theta_n = 1$ if $n = 1$). Note also that the definition of S_0 differs here from other uses: here it represents the initial total stored energy before annealing starts. Primak provides illustrations of a typical activation-energy spectrum (S versus E) and shows how this is modified during isothermal annealing.

The situation for “tempering” (standard rate-of-release measurement) is also analysed for variable activation energies, again with temperature increasing as $T = at$. S as defined here must now become a distribution function and the characteristic annealing function now becomes

$$\Phi = \left[1 - \left((1-n) B \frac{T}{a} E_2 \left(\frac{E}{kT} \right) \right) \right]^{\frac{1}{1-n}}$$

where $E_2(x)$ is one of a class of functions of the form $E_m(x) = x^{m-1} \int_0^\infty u^{-m} e^{-u} du$. Standard

Tables of solutions to these functions are available but for the range of $x, \equiv(E/kT)$, of interest (20-50) it is sufficient to assume that $E_m(x) = (x+m)^{-1} e^{-x}$. The specific application to nuclear graphite appeared in a subsequent paper also by Primak (Ref. [8]). This latter paper is important because it introduces the concept of irradiation annealing, which makes a significant contribution to the distribution of displaced atoms and vacancies at higher irradiation doses. Longer-term irradiation has the effect of diminishing low-temperature peaks in release-rate curves and effectively shifting the energy remaining in the material to positions where its removal requires a higher temperature than would initially have been the case. This is very noticeable in studies of PGA graphite from the commercial Magnox reactors, where often no peak in release is now discernible, with the release curve resembling a monotonic rise to a plateau value. Thus, at higher irradiation doses, particularly approaching those where the accumulation of stored energy is saturating at an equilibrium value (Ref. [9]), the magnitude of a release that can occur at lower temperatures is progressively diminished. This situation does not apply significantly to material from the Piles, although close examination of data in Refs [1] and [2] suggests some indications of the effect. Primak (Ref. [8]) also highlights the importance of irradiation temperature in providing auto-annealing, particularly in the range of activation energies between 2 and 5 eV. For irradiation at 135°C the accumulation is about one half of that at 65°C for the same total dose. He suggests that thermal annealing at these temperatures could only affect damage in the activation-energy range 1.1-1.3 eV and hence that there is a temperature dependency in the irradiation annealing.

The precise nature of the lattice defects introduced by irradiation, which result in the accumulation of stored energy, have been discussed in numerous publications (see, *e.g.*, Ref. [10]). The defects are believed to develop from simple sub-microscopic clusters of a few atoms into interstitial loops of increasingly complex nature. The lattice vacancies begin as monomers, develop into dimers and then into the collapse of regions of layer planes leaving in-plane vacancy loops. A population of sites of different energies results and it is therefore unsurprising that a theory developed on the basis of variable activation energies for annealing of these defects finds greater favour with theoreticians and is consistent with experimental data. This is the essential message of Ref. [5].

It is therefore appropriate to develop further the implications of the variable activation-energy model in addressing the description of Wigner energy still present in Windscale Pile graphite.

2.2. Implications of a Variable Activation Energy

Ref. [11], written shortly after the Windscale accident, attempted to develop the theoretical analysis of Wigner energy and took into account available data from the Hanford facilities in the USA at low irradiation temperature ($\sim 30^\circ\text{C}$) as well as the British data. The Hanford data included higher total doses than the UK data but, over equivalent ranges, behaved in a very similar fashion. This is not surprising since the phenomenon of energy storage occurs at the atomic level, i.e. within the hexagonal lattice, and would not be expected to be influenced by the macrostructure (e.g. porosity, source of filler coke etc.) of the material. This is in contrast to other properties such as dimensional change, strength etc. which are influenced by the physical changes in crystallite dimensions arising from the neutron-damage process. It is stated in Ref. [11] that this insensitivity of Wigner energy to graphite type is also confirmed by reference to early Russian data (Ref.[12]). The Hanford higher dose data clearly demonstrate the approach to overall saturation, and the irradiation annealing effect discussed earlier - as dose increases, the initial low-temperature release peak diminishes and the subsequent plateau value rises. This is described by the authors of Ref. [11] in terms of variable activation energy:

“the increasing overlap of the damaged region of the graphite, this overlapping so changing the annealing activation energies and stored energies of the defects of the peak that the peak is smeared out...”

This effective multiplicity of defect types at the atomic level, each type capable of being located in sites which are differently distorted through interacting lattice stresses, means that *ab initio* calculation of defect energies is unrealistic for even modestly irradiated graphite. Another important point noted in Ref. [11] is the different behaviour under irradiation of virgin graphite compared with that previously irradiated and annealed. This is a low irradiation temperature phenomenon, and arises from the movement of some damage to sites of high activation energy which are not removed by the thermal annealing: their presence then influences the nucleation of new damage sites, which move more easily into further higher-energy sites because of the existing disruption of the graphite lattice.

The authors of Ref. [11] derived a model of stored energy with variable activation energies from the equations given previously. A feature of the model is that for a given rate of temperature rise in an annealing experiment the release of energy from defects with a particular activation energy shows a peak in release rate centred about a particular temperature. The peak arises from the fact that the temperature is increasing, and thus for a time the increase in temperature offsets the decrease in number of residual defects. Therefore with each temperature in the annealing ramp, one can associate a particular energy, the so-called principal activation energy, E . The authors of Ref. [11] also define a value, τ , for the

$$\tau = \frac{1}{\nu \exp(-E/kT)}$$

thermal annealing relaxation time at a temperature, T :

This is closely related to the half life, $(t_{1/2})_i$ at constant temperature T of a defect with an activation energy E_i which is given by $(t_{1/2})_i = 0.693/[\nu \exp(-E_i/kT)]$

The “frequency factor”, ν , is taken by Primak (Ref. [7]) to be $7.5 \times 10^{13} \text{ s}^{-1}$ following work by his colleagues at Argonne National Laboratory. Although it is necessary to turn to experimental data from annealing ramps to derive the distribution of stored energy as a function of activation energy, it is useful to examine the likely lower values of activation energies as a function of temperature from consideration of half lives. Table 1 gives half lives at temperatures in the range of Pile graphite irradiations. From the Table it can be seen that the half lives of defects with activation energies below about 1.2eV are sufficiently short, at around a day ($8.64 \times 10^4 \text{ s}$), even at the lowest graphite irradiation temperatures in the Piles, that a significant population of such defects cannot be sustained. The very small number of such defects, created during the last few days of irradiation, would be expected to decay at ambient temperature over the 40 years or since Pile shutdown, as illustrated by the half lives at 10°C in Table 1

TABLE 1. HALF LIVES OF DEFECTS WITH DIFFERENT ACTIVATION ENERGIES AT DIFFERENT ISOTHERMAL TEMPERATURES

| Activation Energy | 1.1 eV | 1.2 eV | 1.3 eV | 1.4 eV | 1.5 eV | 1.6 eV |
|-------------------|------------|------------|------------|-------------|-------------|-------------|
| Temp | | | | | | |
| 10°C | 3.60(+5)*s | 2.17(+7) s | 1.31(+9) s | 7.92(+10) s | 4.79(+12) s | 2.89(+14) s |
| 25°C | 3.72(+4) s | 1.83(+6) s | 8.97(+7) s | 4.41(+9) s | 2.17(+11) s | 1.06(+13) s |
| 50°C | 1.35(+3) s | 4.91(+4) s | 1.78(+6) s | 6.48(+7) s | 2.36(+9) s | 8.56(+10) s |
| 100°C | 6.75 s | 152 s | 3.40(+3) s | 7.64(+4) s | 1.72(+6) s | 3.85(+7) s |
| 150°C | 0.118 s | 1.84 s | 28.5 s | 444 s | 6.90(+3) s | 1.07(+5) s |
| 200°C | 4.86(-3) | 5.66(-2) s | 0.658 s | 7.65 s | 89.0 s | 1.03(+3) s |
| 250°C | 3.68(-4) s | 3.39(-3) s | 3.12(-2) s | 0.287 s | 2.64 s | 24.3 s |

* $3.60(+5) = 3.60 \times 10^5$
(40 years = $1.3 \times 10^9 \text{ s}$).

As already indicated, in a ramped annealing experiment, energy released from defects with a single activation energy will display a peak in the rate of release with time (or temperature). The temperature at which the peak in release rate occurs varies with ramp rate. The slower the ramp rate, the lower the temperature at which the peak occurs. Essentially this is because more time is available for release at each temperature. The analysis is developed in Reference [13] which derives more explicitly from the Vand/Primak theory a relatively simple but extremely useful equation, relating activation energy, annealing temperature T and the

$$(E_o/kT) + \ln(E_o/kT) = \ln(\nu T/a)$$

ramp rate a, which has been implicitly employed in the earlier work:

The authors of Reference [13] note that the equation should apply to any form of graphite since ‘---- the stored energy is insensitive to the source of the graphite ----’, a point made earlier. The effect of ramp rate on the principal annealing temperature for a particular defect activation energy is illustrated (by use of equation 5) in Table 2 which covers ramp rates of order degrees per minute typical of conventional stored energy determinations. The Table shows that the temperatures for release of principal activation energies in the range 1.3 – 1.6 eV will move up by about 17 -20°C when the ramp rate increases from 2 to 10°C.min⁻¹. This is entirely consistent with Iwata’s observations on samples of lightly irradiated graphite where individual defect types can be distinguished (Ref. [14]), discussed in more detail later.

TABLE 2. PRINCIPAL ANNEALING TEMPERATURES IN DEGREES C (GIVING PEAKS IN RELEASE RATE OF STORED ENERGY) FOR DEFECTS OF DIFFERENT ACTIVATION ENERGIES AT DIFFERENT RAMP RATES

| Activation Energy | 1.1 eV | 1.2 eV | 1.3 eV | 1.4 eV | 1.5 eV | 1.6 eV |
|------------------------|--------|--------|--------|--------|--------|--------|
| 10°C.min ⁻¹ | 84 | 115 | 147 | 178 | 209 | 241 |
| 2°C.min ⁻¹ | 70 | 100 | 130 | 160 | 191 | 221 |
| 1°C.min ⁻¹ | 64 | 94 | 124 | 153 | 183 | 213 |

From the discussion above, which shows that defects with activation energies less than about 1.2 eV should not persist in any number, it can be seen that the temperatures at which the peaks in release would occur for defects with larger activation energies will be greater than about 100°C under normal experimental ramp rates.

This Section has so far considered the implications of a variable activation energy combined with a constant frequency factor. Vand noted (Section 2.1) that the frequency factor might vary but showed that the release expression is far more sensitive to changes in activation energy. In a more recent paper (Ref. [14]) Iwata fitted his data showing a fine structure in the Wigner Energy release spectrum with three Gaussian distributions of activation energies centred on 1.34, 1.50 and 1.78 eV, associated respectively with frequency factors in s⁻¹ of 2.2×10^{12} , 8.5×10^{12} and 1.5×10^{14} . These frequency factors compare with the value of 7.5×10^{13} s⁻¹ used by Primak and by the current authors. Iwata does not discuss the differences in frequency factors arising from his unconstrained fitting exercise. However the data at the different ramp rates can be refitted using an imposed frequency factor of 7.5×10^{13} s⁻¹, with no loss of fit from that derived by Iwata, to give defect activation energies of 1.47, 1.59 and 1.74 eV. This is illustrated in Figure 1 which is based on Figure 3 of Iwata's

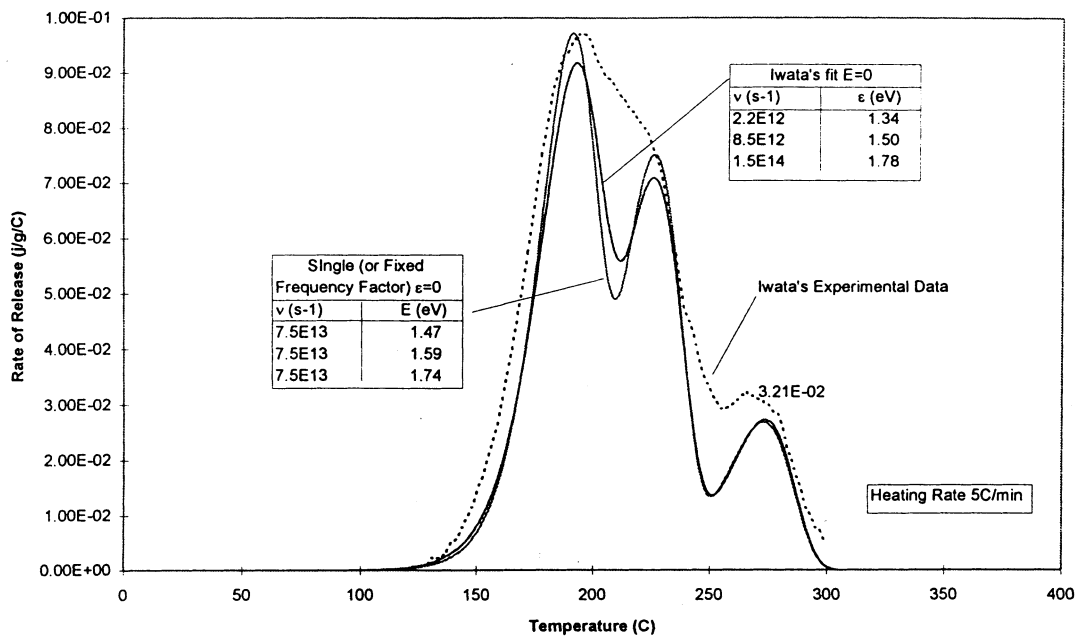


FIG. 1. Comparison of 'pure' activation energies fitted to Iwata's experimental data using the variable frequency factors from Iwata's paper and using a constant frequency factor.

paper. The plot relates to the $5^{\circ}\text{C}\cdot\text{min}^{-1}$ ramp rate and shows the experimental data and Iwata's fit assuming variable frequency factor and 'pure' activation energies, that is no Gaussian spread. Also included on the Figure is a plot with the imposed constant frequency factor and the derived activation energies. This illustrates Vand's assertion that release behaviour is less sensitive to frequency factor than to activation energy.

Iwata's data, as in Figure 1, illustrate a previous point. His specimens were very lightly irradiated, with a total dose of only 4×10^{17} neutrons.cm⁻² ($E > 1$ MeV). Yet, although fine structure was evident in the release curve, to fit the experimental data he had to introduce some spread into his main activation energies. In considering the much more highly irradiated graphite of Pile 1, the need for a multi-activation-energy approach is very evident. The inherent difficulty of predicting defect accumulation from first principles for graphite with all but negligible quantities of damage, is also illustrated by Iwata's data which come from specimens with displacements per atom estimated to be in the range of only $6-8 \times 10^{-4}$ dpa. In contrast the irradiation of Piles graphite is of the order of 10^{21} neutrons.cm⁻², corresponding to about 0.3 dpa.

3. COMPARISON OF STORED ENERGY BEHAVIOUR IN WINDSCALE PILE GRAPHITE WITH THEORY

The preceding section has shown that the description of stored energy and its release behaviour should, in terms of formulation, be no different for Windscale Piles graphite than for other graphite: the total stored energy in a sample can be described by an integral of stored energy distributed among activation energies which have an effective lower limit determined by either irradiation temperature or post irradiation conditions. Also the rate of release is the sum of the individual rates of release from each type of defect, and each release rate will be first order in the remaining number of defects of that type or in remaining amount of stored energy associated with that type of defect. The rate of release equation can be applied to constant temperature or, by tracking residual energy, through periods of varying temperature.

In summary:

$$\frac{dS}{dt} = -v \sum_i S_i(E_i, t) \exp(-E_i/kT)$$

where the initial stored energy S_0 is given by:

$$S_0 = \sum_i S_0(E_i)$$

The need for a variable activation energy description is readily seen from the breadth and location of peaks in the numerous plots of release rate as a function of temperature obtained on trepanned samples from Pile 1 and Pile 2, as illustrated in Figure 2 (Ref. [2]). At $10^{\circ}\text{C}\cdot\text{min}^{-1}$ (the experimental conditions) it can be seen from Table 2 that an increase of 0.1 eV shifts the peak up some 30°C . So peaks or plateaux with widths of 100°C or more point to a wide range of activation energy. This is also shown in Figure 3 by applying a single

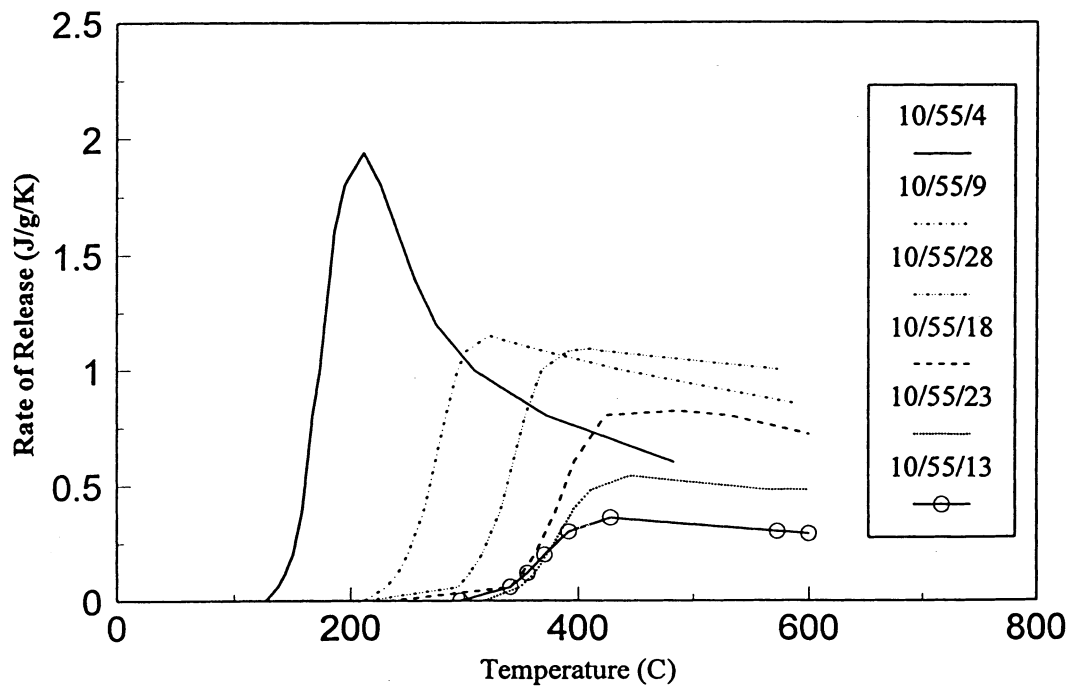


FIG. 2. Stored energy rate of release curves for Pile 1 channel 10/55 BR.

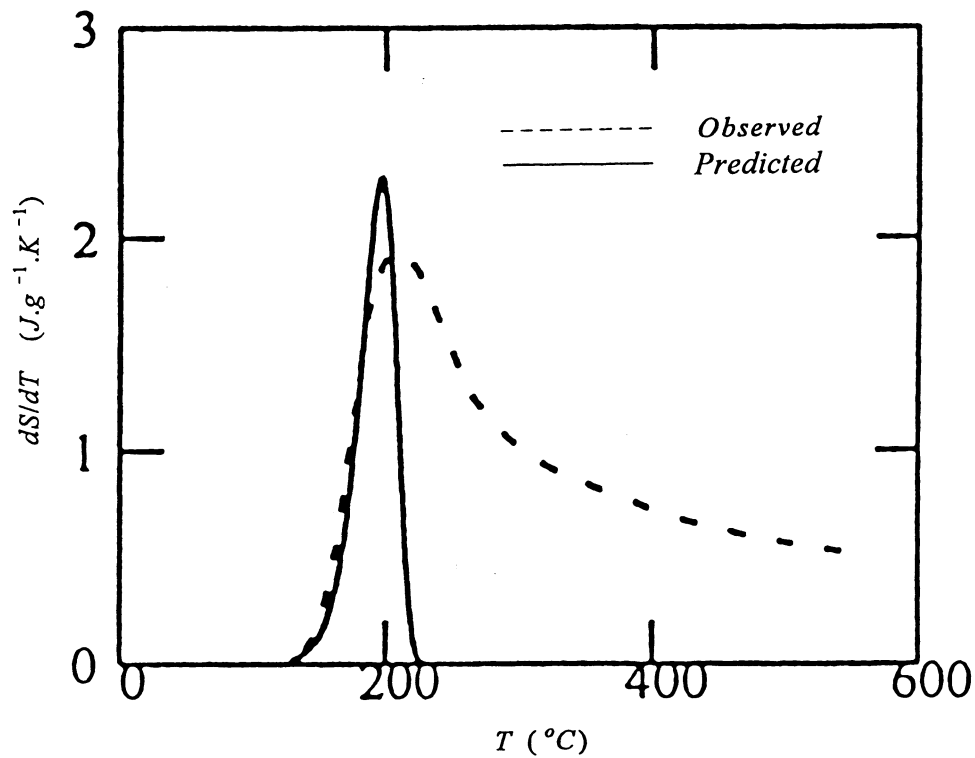


FIG. 3. Observed release of stored energy from Windscale Pile 1 sample 10/55/BR and prediction using a single value of activation energy.

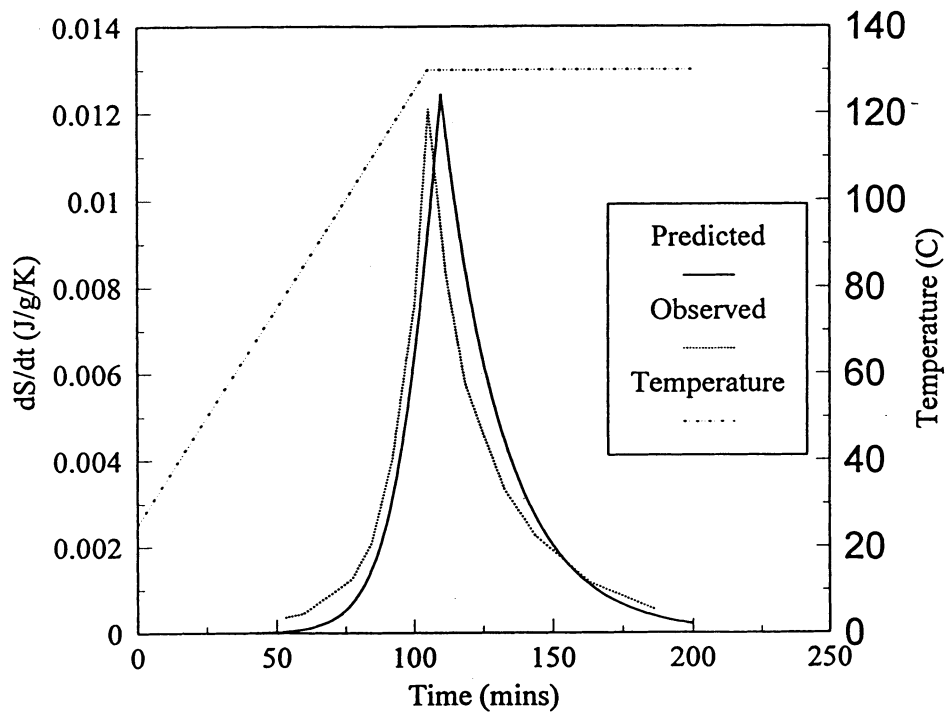


FIG. 4. Observed and predicted release of stored energy from Windscale dowel, sample B12/2.

activation energy model to test against data shown in one of the curves in Figure 2. The ‘prediction’ in Figure 3 assumed a single activation energy of 1.4eV (chosen by trial and error to give a good fit to the rising part of the release curve) and an initial associated stored energy of 500 J.g^{-1} . It is apparent that the prediction follows the experimental observation quite well for the rising portion of the release curve, but the predicted sharp decay in release is not observed. This indicates that the components of release at higher temperatures arise from annealing defects with significantly higher activation energy.

The plots in Figure 2 and the analysis in Figure 3 also illustrate that irradiation temperature influences the nature of the activation energy spectrum. In Figure 2, the brick number increases, as does temperature, from channel inlet to outlet and it can readily be seen that the more easily released, lower activation energy components are progressively missing as irradiation temperature increases. In Figure 3, the fit to the rising part of the curve shows that the sample contained relatively little stored energy with activation energy $<1.4 \text{ eV}$.

The expected first order decay is readily manifest, in samples with one principal activation energy, from release data during isothermal hold periods following ramps, as shown in Figure 4. Here the data have been fitted to a single activation energy of 1.3 eV, derived from isothermal release measurements at several temperatures.

Thus residual stored energy in Windscale Piles graphite conforms to the behaviour expected from the literature.

4. QUANTIFICATION OF THE DISTRIBUTION OF STORED ENERGY IN WINDSCALE PILE GRAPHITE

Past work on the accumulation of stored energy in irradiated graphite has shown that it is very difficult to predict the exact nature of the many types of defect formed and their population densities. This is particularly true of graphite which has a history complicated by intermittent partial annealing as is the case for Windscale Piles graphite. The distribution of stored energy has to be derived from appropriate measurements of the release rate from graphite irradiated to the desired dose and at the required irradiation temperature. It is not possible to extrapolate from a higher irradiation temperature to a lower with any degree of precision.

There are a number of ways to derive the activation energy spectrum from release measurements. There is a method based on that by Primak, in which the experimental release curve, dS/dT , is divided up into vertical strips, I , of width ΔT , and centred on a temperature T_i . The principal activation energy of each strip at T_i is established using equation (6): the value of $S(E_i)$ can then be obtained from

$$S_o'(E_i) = \frac{dS}{dT} \Big|_{T_i} (k + E_i/T_i)^{-l}$$

The initial stored energy, $S_o(E)$, in the vertical strip centred on T_i , is then given approximately by $S_o'(E_i)\Delta E$, where ΔE is the difference in activation energies at the boundaries of the vertical strip, calculated using Equation (6).

Alternatively, with greater numerical effort, one can convert the curve of dS/dT against T , to a curve of $S_o'(E)$ against E using Equations (6) and (9) and integrate directly under the curve to give the stored energy in the range E to $E+\delta E$.

In both methods the fineness of the spectrum of activation energies is arbitrary and needs to be shown to be fit for purpose.

The application, for which a stored energy distribution is derived, is to calculate the rate of release of stored energy under the slow and relatively modest temperature cycles seen in graphite waste packaging and disposal. It is clear that defects with low activation energies will be released but that defects with high activation energies will not be released at a significant rate. As has already been discussed, there is effectively a lower limit on activation energy based on defect lifetime at irradiation (and subsequent storage) temperatures close to ambient. This is likely to be about 1.2 eV. It is relevant in this context to recall (Table 2) that the peak in release rate for such a defect will be at about 100-115°C for ramp rates of 2-10°C.min⁻¹. The experimental data show that relatively small amounts of energy can be detected at these temperatures. The highest activation energies of interest depend on the waste packaging and repository temperature cycles: it has been shown that the slower the cycle the lower the temperature at which complete energy release associated with a particular defect type will occur during the cycle. (The release rates may however be very low.)

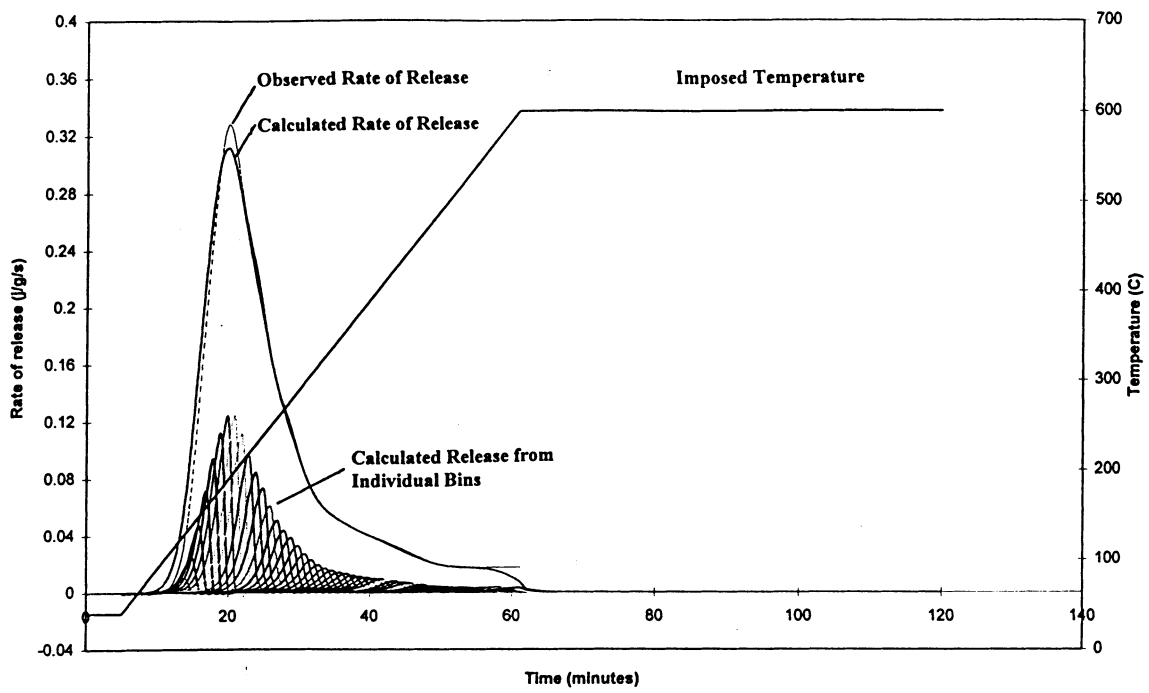


FIG. 5. Fitting of energy distribution to data from Windscale pile 2 dowel, B12/2 sample E/3 at 10 °C/min.

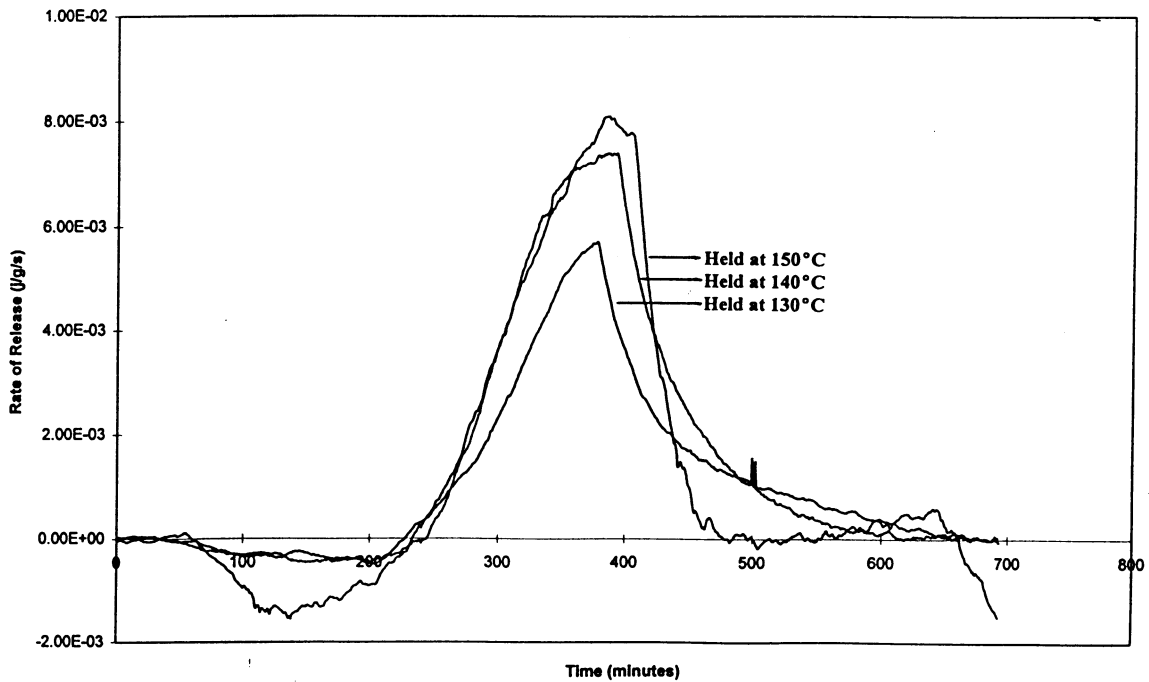


FIG. 6. Release rate from B12/2 during ramps of 0.3 °C/min followed by isothermal holds measured by Preston and Melvin [2].

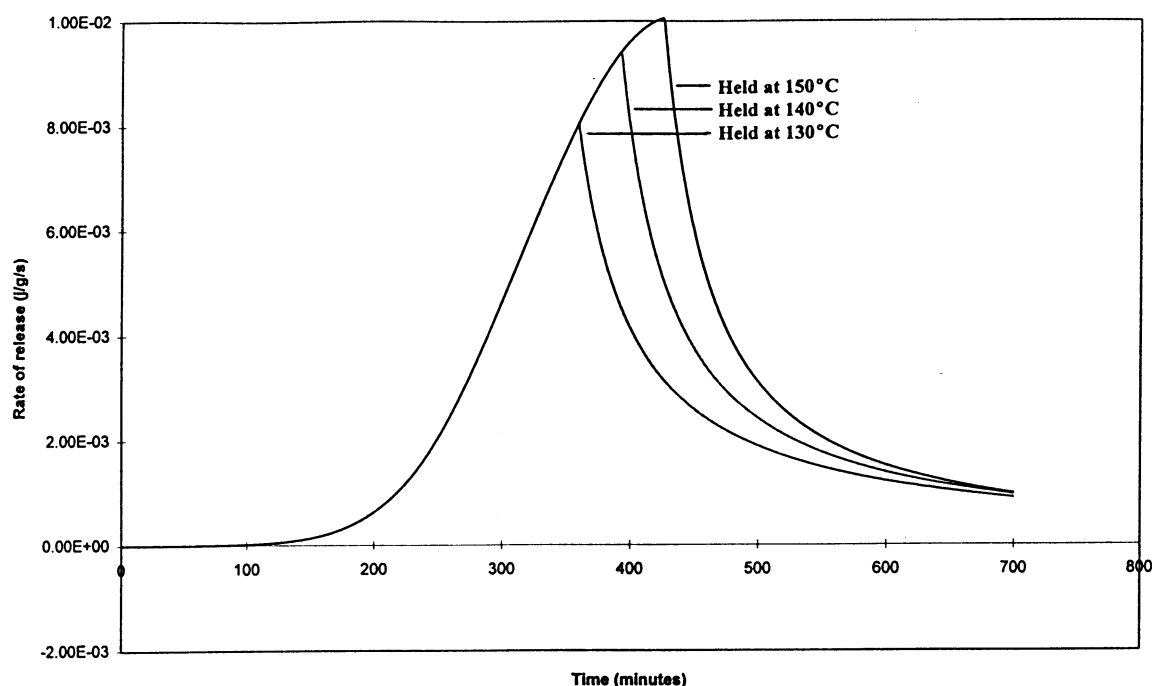


FIG. 7. Release rate during ramps of 0.3 °C/min followed by isothermal holds predicted for the experimental curves in Fig. 6.

TABLE 3. COMPARISON OF MEASURED ENERGY RELEASES DURING RAMP AND HOLD TESTS FROM PRESTON AND MELVIN [3] WITH PREDICTIONS FROM DECONSTRUCTION OF FULL RELEASE RATE CURVE.

| Dowel sample ID | Ramp rate K/min | Hold temp ° C | Measured release (J/g) | | | Predicted release (J/g) (from energy distribution in sample E/3 ramped at 10K/min) | | |
|-----------------|-----------------|---------------|------------------------|-------|-------|------------------------------------------------------------------------------------|-------|--------|
| | | | ramp | hold | Total | Ramp | Hold | Total |
| A/2 | 1 | 150 | 31.5 | 34.4 | 65.9 | 41.45 | 55.21 | 96.66 |
| B/2 | 1 | 140 | 20.1 | 24.4 | 44.5 | 27.03 | 50.48 | 77.51 |
| B/5 | 1 | 130 | 11.2 | 14.8 | 26.0 | 15.92 | 42.77 | 58.69 |
| C/2 | 1 | 120 | 1.70 | 16.3 | 18.0 | 8.31 | 33.15 | 41.46 |
| D/3 | 0.3 | 150 | 40.34 | 10.56 | 50.90 | 62.19 | 43.87 | 106.06 |
| B/3 | 0.3 | 140 | 36.97 | 22.10 | 59.07 | 44.4 | 43.6 | 88.0 |
| C/3 | 0.3 | 130 | 20.5 | 21.12 | 41.62 | 28.74 | 40.61 | 69.35 |

Thus the quantitative distribution of stored energy in a graphite sample derived from a rapid rate of release experiment can be used to predict how Wigner energy in the same piece of graphite will be released under a different temperature cycle. With regard to Piles graphite there is a good data base on stored energy. The choice of data for a safety case is outside the scope of this paper.

To provide assurance of the robustness of the stored energy derivation and application procedure, some checks have been conducted within the available database. Since specimens in general only undergo one energy release test, it is first necessary to check on the reproducibility of behaviour in specimens cut from a single piece of graphite. Once this has been done satisfactorily, sets of data on adjacent specimens tested under differing ramp rates can be examined. Data from specimens ramped at common ramp rate but subject to isothermal holds at different points on the ramp make a useful set. Data from Reference [3] in which samples were cut from a single irradiated dowel, identified as B12/2, have been used for a checking exercise and results are illustrated in Figures 5, 6 and 7.

Figure 6 shows the rate of release vs time plot for sample E/3 taken at $10^{\circ}\text{C}\cdot\text{min}^{-1}$ up to 600°C . The curve has been analysed as described above to give a distribution of stored energy. The rate of release from the individual components of this distribution have also been plotted on Figure 6, and the sequential ‘emptying’ of energy ‘bins’ can be seen as the temperature ramp (also plotted) progresses. The energy distribution has then been used to predict the behaviour of neighbouring samples from the dowel which were taken at a common ramp rate to different temperatures and held there. Figure 6 allows the experimental data to be compared with prediction in Figure 7 for samples ramped at $0.3^{\circ}\text{C}\cdot\text{min}^{-1}$ and held at 130, 140 and 150°C . The experimental data show reasonable sample-to-sample reproducibility in terms of the gradient on the ramp part. The predictions naturally have a common behaviour on the ramp part with the slope predicted well (this is the correction for ramp rate from Figure 5). The pattern of the experimental data is reproduced well, considering that the experimental data suffer from some drift on the base line. Table 3 compares the observed and predicted release of energy during the ramp, during the hold and in total for the tests illustrated in Figure 6 and for similar ones on samples from the same dowel but where the ramp rate was 1 rather than $0.3^{\circ}\text{C}\cdot\text{min}^{-1}$. The predicted releases are generally rather larger than those observed, but the experimental base line may affect the integration of experimental data. However, the sample to sample behaviour is again generally consistent in that samples ramped and held at lower temperatures release less energy than those taken to higher temperatures.

Thus samples cut from a single dowel show reasonable reproducibility of behaviour on common ramps, and the quantitative stored energy distribution derived from a full ramp can be used to predict the behaviour of neighbouring samples subjected to different temperature cycles.

5. ENERGY RELEASE PREDICTIONS UNDER SLOW, LOW-TEMPERATURE CYCLES

The previous section illustrated how stored energy distributions could be derived and shown to be internally consistent within a data set. The data are obtained under conditions where multiple peaks are not seen. The ramp rates relevant to waste packaging and disposal are slow such that the energy release from defects of different types will be more spread out. As has already been mentioned the fineness of the energy spectrum derived from deconstructing the rate of release curve needs to be fit for purpose. The smoothness of the experimental rate of release curve taken together with the coarse and fine fits illustrated in Figure 5 indicates that the activation energy spectrum, if not continuous, is discretised in increments of less than about 0.05eV in the relevant region. The finer fit, discretised in increments of $0.03 - 0.05\text{eV}$ (Table 4) produces a smooth curve when the bins are summed.

TABLE 4. COARSE AND FINE STORED ENERGY SPECTRA USED TO FIT DATA FOR DOWEL FROM PILE 2 CHANNEL 22/67 [14]

| Coarse Spectrum | | Fine Spectrum | |
|-------------------------|------------------------------------|-------------------------|------------------------------------|
| Activation Energy eV | Stored Energy J.g ⁻¹ | Activation Energy eV | Stored Energy J.g ⁻¹ |
| | | 1.072 | 0.2 |
| | | 1.116 | 1.7 |
| 1.117 | 3.6 | 1.160 | 4.2 |
| | | 1.198 | 7.3 |
| 1.199 | 13.9 | 1.233 | 10.7 |
| 1.269 | 27.0 | 1.268 | 14.3 |
| | | 1.307 | 15.7 |
| 1.326 | 33.1 | 1.335 | 17.3 |
| | | 1.367 | 21.1 |
| 1.399 | 36.7 | 1.399 | 18.5 |
| | | 1.420 | 17.9 |
| 1.449 | 45.0 | 1.449 | 22.8 |
| | | 1.487 | 24.0 |
| 1.526 | 42.4 | 1.525 | 21.4 |
| | | 1.564 | 16.0 |
| 1.593 | 33.7 | 1.593 | 17.0 |
| | | 1.648 | 19.3 |
| | | 1.707 | 15.8 |
| 1.763 | 48.7 | 1.762 | 14.6 |
| | | 1.832 | 7.5 |
| 1.887 | 21.2 | | |
| | Total 305 | | Total 287 |

Both the coarse and fine fits (from Table 4) have been applied to temperature cycles rising from 20°C to 100°C, held constant, and then declining. In the one case the rise occurs over a day, with a hold for 2 days and a fall over another day, and in the second case the rise is over 5 days with a 10 day hold and a 5 day fall. The results are shown, for the fine fits, in Figures 8 and 9.

For each cycle the coarse fit still gives a release rate with peaks or shoulders, and the finer fit gives a smoother curve. The energy released during the ramp and hold is very similar for both fits. It is also instructive to compare the same fit under the ½/1 day and 5/10/5 day cycles. For ease of visual comparison the release rates have been plotted on the same scale. During the ramp period more ‘bins’ are emptied in the slower cycle, and hence more energy released, but in both cases many of the bins, shown in Table 3, remain effectively untapped. In the hold period at the common temperature of 100°C rather more energy is released in the ½/1 day cycle because bins with lower activation energies (shorter half lives) are contributing, these bins having been emptied on the ramp in the 5/10/5 day cycle. In total the slower the cycle the more energy is released, but the rate of release is very much reduced. It can also be seen by comparison of Figures 8 and 9 that although the cycle time is extended, the way in which the releases from adjacent bins overlap is maintained. Discretisation of the activation energy distribution in increments of about 0.03-0.05 eV is adequate to avoid predictions of energy release in low cycles being compromised by too coarse a fit.

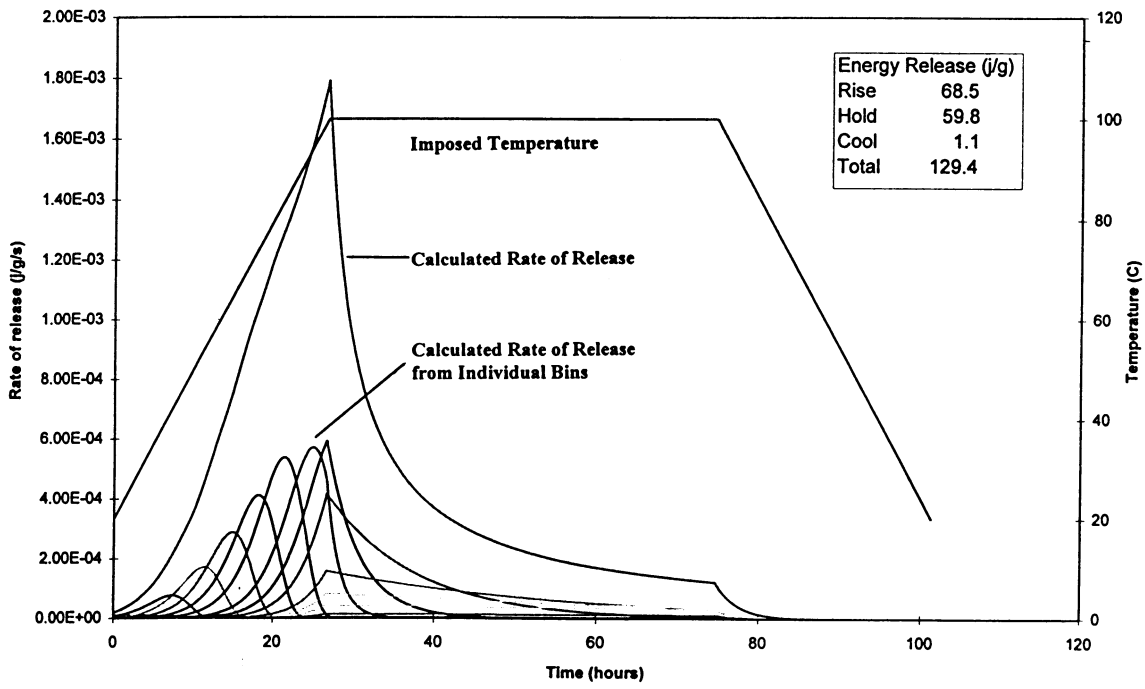


FIG. 8. Predicted energy release in a 4 day cycle using the fine spectrum from table 3.

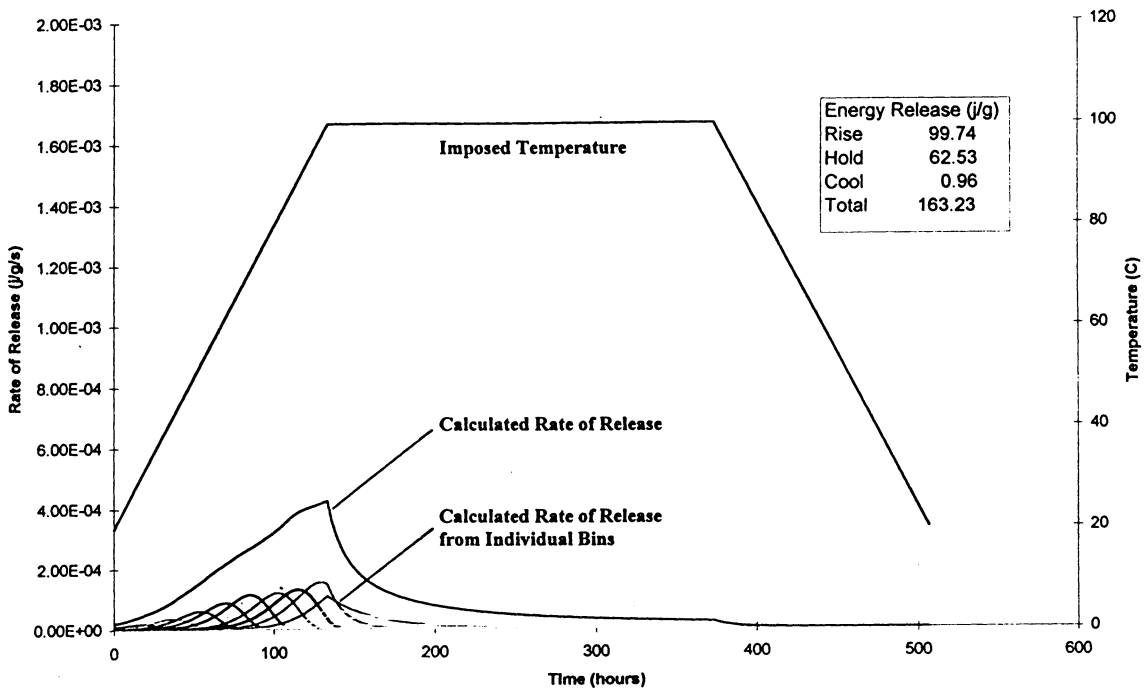


FIG. 9. Predicted energy release in a 20 day cycle using the fine spectrum from table 3.

The examples above clearly use an imposed temperature cycle, and do not consider the way in which local temperatures can be modified as a result of energy release. This is handled by a feed back loop into the release rate Equation 7 coded as a subroutine into thermal modelling codes, and is not part of this paper.

6. VALIDATION OF RELEASE PREDICTIONS AT LOW TEMPERATURE

The fundamental understanding of Wigner energy gives no reason to suppose that releases at low temperatures over long times should not proceed according to Equation 7, and as predicted in Section 5. Clearly the predictions assume bins behave independently of each other and assume that for example relaxation of one region of a lattice does not affect the activation energy required for release of remaining defects, i.e. there is no ‘trickle down’. It also ignores the aggregation of defects during annealing to produce complexes with higher activation energies. The very large spread in activation energies, with many defects effectively very difficult to dislodge at low temperatures suggests this defect/defect interaction will not have a large effect on release rates. Some validation of predictions over longer timescales would however provide additional confidence in the use of the methodology for safety case applications.

After consideration of the experimental difficulties in measuring the heat release directly in long low cycles, and recognising the reasonable degree of consistency in behaviour of samples cut from a single piece of graphite (Section 4), an achievable test of the predictions is proposed as follows. Cut several samples from a single piece of Pile graphite, core or debris. The irradiation history need not be known as long as the graphite retains stored energy releasable at low temperatures. Take one or two samples through the conventional ramp experiment to determine rate of release with temperature or time, the ramp rate (probably less than 10 K.min^{-1}) being suitable for deconstruction of the release rate curve to give a stored energy distribution as described. Use this distribution to identify, by prediction, time/temperature cycles which will release suitable (see later) amounts of energy. Expose the samples to these cycles, measuring only time and sample temperature, and then take the samples through the same conventional ramp experiment and deconstruct the resulting curves as before. Compare the predicted releases during the time/temperature cycles with the difference between ‘before’ and ‘after’ ramp-rate experiment data and derived stored energy distributions. It can now be seen that ‘suitable’ time/temperature cycles are those which will make a readily measurable difference to the output from the conventional experiment. In this sense, suitable time/temperature conditions cannot be identified until the initial stored energy distribution is known.

7. CONCLUSIONS

A review of the classical theories on the accumulation and release of Wigner energy from irradiated graphite, together with an analysis of past and present data from the graphite of the Windscale Piles, shows that the behaviour of the Piles graphite is consistent with the existence of a distribution or spectrum of “activation energies” associated with the sites of displaced atoms and vacancies.

The form of the release of stored energy is essentially independent of graphite type, but the precise irradiation history (temperature, dose) and the occurrence of annealing activities, leads to a unique distribution of remaining stored energy in the graphite from the Windscale core which cannot be predicted reliably from first principles.

The lower the irradiation temperature, the lower the characteristic activation energies associated with damage sites which can retain “stored” energy. However, as irradiation continues, some displaced atoms and lattice vacancies (or the clusters of atoms or vacancies derived from them) are shifted to positions of higher activation energy, requiring much higher annealing temperatures to release the associated energy: indeed, to release *all* stored energy from an irradiated graphite sample, a temperature in excess of 2000°C would be necessary. The temperatures necessary to release energy from these higher levels are not accessible in storage or during grouting cycles and only the energy in the lowest remaining activation-energy sites could potentially be released over these timescales.

Energy associated with sites from which release was possible at the temperature of irradiation can only be present in an extremely low concentration resulting from the steady-state balance of formation *versus* annealing which was “frozen in” when irradiation ceased, and are not of significance in the present context.

In the context of storage and disposal of this graphite, total stored energy is not relevant: one only needs to consider the energy in sites capable of release at the temperatures of grouting and storage which include the effects of an additional temperature rise as a result of energy feedback into the system. Since the temperature cycles associated with these activities lie below those traditionally used in determinations of the rate of release of stored energy, it is necessary either to extrapolate data to lower temperatures, or to obtain new data.

A method to deconvolute rate of release curves obtained for representative Pile-1 graphite samples in order to identify the initial activation-energy distribution of the stored energy has been described. The initial activation energy distribution derived from measurements on one sample can be used to predict successfully the energy release behaviour of neighbouring samples exposed to different temperature cycles.

The required fineness of the observed energy distribution has been examined in the context of the long, low temperature cycles applicable to waste grouting and disposal.

It is considered prudent to validate the predictions of energy release from the calculational route by means of experimental measurements. A method of providing an achievable test of the predictions is proposed.

ACKNOWLEDGEMENTS

This work was funded by BNFL, Waste Management and Decommissioning at Sellafield. The authors wish to acknowledge helpful discussions with Dr K A Simpson and thank I. Boughey for carrying out many of the calculations.

REFERENCES

- [1] Preston, S.D. and Melvin, G.T., Results from the 1997/98 Stored Energy Survey of Windscale Pile 1, AEA Technology plc Report AEAT-3400, WPTC(98)P73 (1998).
- [2] Preston, S.D., Melvin, G.T. and Charles, R., Results from the 1996/97 Stored Energy Survey of Windscale Pile 2, AEA Technology plc Report AEAT-1464, WPTC(97)P64 (1998).

- [3] Preston, S.D. and Melvin, G.T., Rate of Release Measurements at Various Heating Rates on Samples from a Windscale Pile 2 Graphite Dowel, AEA Technology plc Report AEAT-3169 (1998).
- [4] Data Sheet C7/1, Compendium of CAGR Core Data and Methods, Nuclear Electric Report GCDMC/P28 (CSDMC/P28) (1994).
- [5] Kelly, B.T., Modelling of the Kinetics of Release of Wigner Energy in Graphite, UKAEA Report NRL-R-2028(S) (1989).
- [6] Vand, V., A Theory of the Irreversible Electrical Resistance Changes of Metallic Films Evaporated in Vacuum, Proc. Royal Society (London), **A55**, (1943) 222-246.
- [7] Primak, W., Kinetics of Processes Distributed in Activation Energy, Physical Review, **100**,(1955) 1677-1689.
- [8] Primak, W., Fast-Neutron Damaging in Nuclear Reactors: Its Kinetics and the Carbon Atom Displacement Rate, Physical Review, **103**, (1956) 1681-1692.
- [9] Kelly, B.T., Brocklehurst, J.E. and Gilchrist, K.E., Stored Energy in Irradiated Graphite, BNFL Memorandum No. 1502, (1978).
- [10] Kelly, B.T., Radiation Damage in Graphite and its Relevance to Reactor Design, Progress in Nuclear Energy, **2**, (1978) 21-269.
- [11] Bridge, H., Kelly, B.J. and Gray, B.S., Stored Energy and Dimensional Changes in Reactor Graphite, UKAEA Report TRG 119 (C), (1961).
- [12] Klimenkov, V.I. and Aleksenko, Yu. N., "Changes in the Properties of Graphite when Irradiated by Neutrons, USSR Academy of Sciences Physics 2, (1956) 226 et seq..
- [13] Kelly, B T and Preston, S D, "Assessment of Irradiation Damage in the DIDO Graphite Reflector, UKAEA Report SL-CON-120.
- [14] Iwata, T, Fine Structure of Wigner Energy Release Spectrum in Neutron- Irradiated Graphite, Journal of Nuclear Materials, **133+134**, (1985) 361-364.
- [15] Bell, J.C. and Gray, B.S., "Stored Energy Studies made on Windscale Pile Graphite since October 1957, UKAEA Report TRG 84 (W), (1961).